

JAAS

Accepted Manuscript



This article can be cited before page numbers have been issued, to do this please use: C. Cerutti, C. Sánchez, R. Sánchez, F. Ardini, M. Grotti and J. Todoli Torro, *J. Anal. At. Spectrom.*, 2018, DOI: 10.1039/C8JA00391B.



This is an Accepted Manuscript, which has been through the Royal Society of Chemistry peer review process and has been accepted for publication.

Accepted Manuscripts are published online shortly after acceptance, before technical editing, formatting and proof reading. Using this free service, authors can make their results available to the community, in citable form, before we publish the edited article. We will replace this Accepted Manuscript with the edited and formatted Advance Article as soon as it is available.

You can find more information about Accepted Manuscripts in the [author guidelines](#).

Please note that technical editing may introduce minor changes to the text and/or graphics, which may alter content. The journal's standard [Terms & Conditions](#) and the ethical guidelines, outlined in our [author and reviewer resource centre](#), still apply. In no event shall the Royal Society of Chemistry be held responsible for any errors or omissions in this Accepted Manuscript or any consequences arising from the use of any information it contains.

Journal Name

ARTICLE

Determination of trace elements in undiluted wine samples using an automatized total sample consumption system coupled to ICP-MS

Received 00th January 20xx,
Accepted 00th January 20xx

DOI: 10.1039/x0xx00000x

www.rsc.org/

Claudia Cerutti,^a Carlos Sánchez,^b Raquel Sánchez,^{b,*} Francisco Ardini,^a Marco Grotti,^a José-Luis Todolí^b

A novel method for the elemental analysis of undiluted wine samples was optimized and validated. The method was based on the use of a high-temperature torch integrated sample introduction system (hTISIS) coupled to inductively coupled plasma mass spectrometry (ICP-MS). The operating conditions (hTISIS temperature and liquid flow rate) were optimized in terms of sensitivity and matrix effects. Low liquid flow rates allowed to continuously introduce organic samples into the plasma source with minimum soot as well as salty deposits formation at the ICP-MS interface and/or plasma thermal degradation. A double pass Scott-type spray chamber thermostated at 2°C was taken as the reference sample introduction system. The results indicated that the hTISIS operated at 125°C and 30 $\mu\text{L min}^{-1}$ as liquid flow rate improved the sensitivity and mitigated the extent of matrix effects compared to the conventional system. Once the optimum conditions were selected, the method was validated and applied to the determination of sixteen trace elements (Ti, V, Cr, Mn, Fe, Ni, Cu, Zn, As, Mo, Cd, Nd, Sm, Gd, Tb and Pb) in ten real wine samples. The sample was merely aspirated to the nebulizer with no additional preparation. For the sake of comparison, the samples were microwave digested and analyzed using a conventional setup. Method detection limits achieved by the hTISIS were from 2 to 40 times lower than those found using the standard procedure and ranged from 0.002 to 6 $\mu\text{g kg}^{-1}$. Furthermore, the accuracy of the quantification using the hTISIS was not significantly different as compared to that afforded by the conventional procedure and substantially improved in comparison with the direct analysis of wine using a Scott spray chamber. Sample throughput was close to 10 h^{-1} that was in clear contrast with 2 h^{-1} , estimated when the digestion method was used. Finally, the suitability of the developed method for the routine analysis of wine samples was demonstrated by performing a 20-hours long analysis sequence. Good signal stability and accurate results were obtained for ten representative Italian and Spanish wines.

Introduction

Wine is an alcoholic beverage widely consumed throughout the world, having important social and economic impacts. From a chemical point of view, wine is a complex mixture, containing water, ethyl alcohol, sugars and a great variety of other organic and inorganic compounds, whose content is related to the grape variety, production area (soil and climate), yeast type, production, transport and storage procedures.¹

Complementarily to other parameters, wine elemental composition can provide relevant information on its quality, characteristics and origin.²⁻⁵ Metals, such as Cu, Fe, Mn, Ni and Zn mainly affect the organoleptic characteristics of wine (*i.e.*, flavor, freshness, aroma, color and taste), due to the formation

of precipitates (yeast, fining and filtration sediments) or clouding during wine fermentation, maturation and storage.^{3,6} Other elements, including As, Cd, Cu, Pb and Zn, are of great concern due to their toxicity.⁶ Metals origin can be classified in endogenous and exogenous. Endogenous metals come from the soil which vines are grown on and they are delivered to the wine through grapes. On the other hand, exogenous metals are associated with external impurities that can contaminate the wine during growth of grapes or at different stages of winemaking, from harvesting to bottling and cellaring.

The official methods for the determination of metals in wine, commonly applied in routine laboratories, are based on atomic spectrometry,^{3,7,8} including flame atomic absorption spectrometry (FAAS),^{3,7-14} graphite furnace atomic absorption spectrometry (GFAAS),^{3,7,8,15,16} inductively coupled plasma optical emission spectrometry (ICP-OES),^{3,7,8,17-22} and inductively coupled plasma mass spectrometry (ICP-MS),^{3,5,7,8,17,23-31} being the latter the most applied technique in recent years. However, the introduction of organic samples into the plasma source is still a challenge as ICP techniques suffer

^a Department of Chemistry and Industrial Chemistry
University of Genoa
Via Dodecaneso 31, 16146 Genoa, Italy

^b Department of Analytical Chemistry, Nutrition and Food Science
University of Alicante
P.O. Box 99, 03080, Alicante, Spain
e-mail: r.sanchez@ua.es

from severe interferences caused by complex organic matrices, including matrix effects, plasma degradation and soot deposition at the injector tip and interface cones.^{32,33,34} To circumvent them, several sample preparation approaches have been developed, such as sample dilution,^{7,22,35,36,37,38,39,40,41} conventional dry/wet sample digestion,^{7,36,42} microwave- or ultraviolet-assisted acid digestion,^{7,10,19,22,43,44,45} dealcoholisation^{7,42} and analyte separation.⁷ However, all these methods show some problems caused by the addition of reagents, potential sample contamination and degradation of limits of detection, among others.

As an alternative to these approaches, the use of the high temperature torch integrated sample introduction system (hTISIS) has been proposed and successfully applied for the analysis of complex matrices.^{46,47,48,49} The basic principle of this low sample consumption system relies on the achievement of complete aerosol evaporation before its introduction into the plasma source, thus accomplishing analyte transport efficiency close to 100% regardless the sample matrix. This point allows applying the so-called universal calibration.^{46,50,51} However, a too high amount of solvent reaching the plasma may degrade its thermal characteristics. Therefore, low sample flow rates (*i.e.*, on the order of a few tens of microliters per minute) should be selected when using the hTISIS under continuous sample aspiration regime. Additional advantages of the hTISIS over conventional sample introduction systems have been reported, including the improvement of sensitivity and limits of detection and the shortening of wash out times. This sample introduction system has been successfully applied for carrying out the determination of metals in a wide range of complex organic matrices, among them bioethanol samples, making possible the removal of matrix effects from 0 to 100% of ethanol in ICP-OES⁵² and from 0 to 50% in ICP-MS⁴⁸ (*i.e.*, sensitivity virtually equal for different ethanol-water mixtures). It should be noted that most wine samples contain ethanol at concentrations typically up to around 15% (v/v), although other organic compounds such as sugars or carboxylic acids as well as salts are present.

Normally, the methods proposed for the elemental analysis of wine samples involve a dilution factor included within the 1:2-1:20 range.^{22,35,36,37,38,39,40,41} The main goal of the present work was thus to develop a novel procedure for the direct quantification of sixteen elements in wine samples, based on the combination of the hTISIS with an ICP-MS instrument. Studies aimed at validating the conceived method by comparison with a conventional digestion procedure and evaluating the analytical figures of merit were also considered in the frame of this study. A final objective of this study was to try to test the adaptability of the hTISIS to an automatized ICP-MS analysis procedure.

Experimental

Standard solutions and samples

10 mg L⁻¹ multi-element standard SCP33MS (SCP Science, Quebec, Canada) and 10 mg L⁻¹ rare earth ICP-MS standard CMS-1 (Inorganic Ventures, Christiansburg, VA, USA) were used as analyte stock solutions. Additionally, 1000 mg L⁻¹ Ge and Re

standard solutions (HPS, Charleston, SC, USA) and 1000 mg L⁻¹ Rh standard solution (SCP Science) were used as internal standard stock solutions. Standards were daily prepared by serial dilution in 10% (v/v) ethanol using ultrapure water (Millipore, El Paso, TX, USA) and analytical-grade 96% ethanol (Panreac, Barcelona, Spain). The analyte concentrations ranged from 0.5 to 500 µg kg⁻¹ (0.05 to 50 µg kg⁻¹ for rare earth elements) and the concentration of the internal standards was 40 µg kg⁻¹.

The following Italian and Spanish wine samples were analyzed: Gutturino (red), ethanol content: 12% v/v; Malvasia (white), ethanol content: 11% v/v, and Ortrugo (white), ethanol content: 11% v/v, from Piacenza (Italy); Cabernet Sauvignon (red), ethanol content: 13% v/v, and Cortese (white), ethanol content: 14% v/v, from Tortona (Italy); Monastrell (red), ethanol content: 13% v/v, and Tempranillo (red), ethanol content: 14% v/v, from Alicante (Spain); ecological wine (red), ethanol content: 14% v/v, from Rioja (Spain) and ecological wine (red), ethanol content: 13.5 % v/v, from Alcoy (Spain). Wine samples were filtered on 0.45-µm PTFE membranes (Filabet, Barcelona, Spain). One sample (Gutturino red wine) was spiked at the concentration of 50 µg kg⁻¹ and used for method optimization.

Instrumentation

The instrument used was an Agilent Technologies (Santa Clara, California, USA) 7700x ICP-MS spectrometer, equipped with a high matrix introduction system (HMI) and the collision-reaction cell (CRC) operating in KED mode (He). The main operating conditions are gathered in Table 1.

The sample introduction system was the hTISIS, constituted by a MicroMist nebulizer (Glass Expansion, Melbourne, Australia) with EzyFit sample connector and EzyLok argon connector, jointed to a 9-cm³ single-pass spray chamber, heated by means of a copper coil. The setup was equipped with a thermocouple to control the chamber walls temperature.⁴⁶ The hTISIS was operated in continuous sample aspiration mode and the liquid flow rate was optimized in the 20-50 µL min⁻¹ range. A double pass Scott-type spray chamber thermostated at 2°C was taken as the reference system for the analysis of the undiluted samples. In this case, the liquid flow rate was 100 µL min⁻¹.

In order to perform the analysis of real wine samples, they were automatically delivered to the nebulizer by means of the Agilent G3160B autosampler, using 0.25-mm flared end PVC tubing (Glass Expansion, Melbourne, Australia).

Microwave-assisted acid digestion

For comparison, the wine samples were also treated using the microwave digestion system Start D (Milestone, Sorisole, Italy). Approximately 0.7 g of each sample, weighed with a precision of ±0.1 mg, were transferred to the microwave digestion vessels and then 7 mL of 65% HNO₃ and 1 mL of 30% H₂O₂ were added. The temperature was increased from room temperature to 200 °C at a constant rate of 12 °C min⁻¹ and kept at this value for 15 min. The resulting solutions were transferred to volumetric flasks and made up to 10 mL with ultrapure water.

Table 1. ICP-MS operating conditions

Sample introduction system (hTISIS)	
Liquid flow rate/ $\mu\text{L min}^{-1}$	20-50
Temperature/ $^{\circ}\text{C}$	50-300
Nebulizer gas flow rate/ L min^{-1}	0.4
Ar HMI flow rate/ L min^{-1}	0.56
Plasma	
Plasma gas flow rate/ L min^{-1}	15.0
Auxiliary gas flow rate/ L min^{-1}	1.0
RF Power/W	1600
Collision cell	
He flow rate/ mL min^{-1}	4.3
OctP Bias/V	-18
Oct RF/V	200
Energy discrimination/V	3.0
Acquisition parameters	
Number of replicates	5
Integration time/s	0.3
Sweeps per replicate	100
Measured ions	
Analytes	$^{47}\text{Ti}^+$, $^{51}\text{V}^+$, $^{52}\text{Cr}^+$, $^{55}\text{Mn}^+$, $^{56}\text{Fe}^+$, $^{60}\text{Ni}^+$, $^{63}\text{Cu}^+$, $^{66}\text{Zn}^+$, $^{75}\text{As}^+$, $^{95}\text{Mo}^+$, $^{111}\text{Cd}^+$, $^{146}\text{Nd}^+$, $^{147}\text{Sm}^+$, $^{157}\text{Gd}^+$, $^{159}\text{Tb}^+$, $^{208}\text{Pb}^+$
Internal standards	$^{72}\text{Ge}^+$, $^{103}\text{Rh}^+$, $^{185}\text{Re}^+$
Diagnostics	$^{140}\text{Ce}^+$, $^{140}\text{Ce}^{++}$, $^{140}\text{Ce}^{16}\text{O}^+$

Results and discussion

Optimization of hTISIS conditions

Effect of hTISIS temperature and liquid flow rate on sensitivity

As previously reported for the ICP-MS analysis of other complex matrices by hTISIS,^{46,48,49} the spray chamber temperature and the liquid flow rate are crucial variables, significantly affecting both the sensitivity and matrix effects. To evaluate the effect of these parameters on sensitivity for this specific matrix, a non-diluted wine sample was spiked with the multielement solution at a $50\mu\text{g kg}^{-1}$ concentration and the ion intensity was measured for various nuclides at temperatures ranging from 50°C to 300°C . The experiment was performed at three liquid flow rates (20, 30 and $50\mu\text{L min}^{-1}$). The intensities obtained at each temperature were normalized with respect to those obtained using the Scott spray chamber, taken as the reference system ($100\mu\text{L min}^{-1}$). The results for three representative ions

(covering the mass range from 55 to 208 amu) are reported in Figure 1. It was observed that, at a given liquid flow rate, the ion intensity increased with the hTISIS temperature, reaching a plateau at $125\text{-}150^{\circ}\text{C}$. Under these conditions, the sensitivity was from 2 to 6-times higher than that obtained with the reference system, despite the 2 to 5-times lower liquid flow rate set for the hTISIS. This was clearly a consequence of the improvement in the droplet evaporation inside the hTISIS, thus increasing the total mass of analyte reaching the plasma, as previously observed for bioethanol samples.⁴⁸

A further increase in temperature led to a drop in the signals. A possible explanation for this trend could be based on a degradation of the plasma thermal state. However, by measuring the doubly charged and oxide ions at different temperatures, it was concluded that no any significant change in the plasma ionization conditions occurred. Therefore, the drop in sensitivity was likely due to changes in the ion spatial distribution in the plasma.⁴⁸ According to this mechanism, at high hTISIS temperatures, the aerosol evaporation became more efficient. Therefore, the solvent was delivered to the plasma in vapor form and ions were generated upstream the plasma. This gave rise to an enhanced chance for ion transversal diffusion. As a small plasma volume is sampled in ICP-MS, the ion sampling efficiency from the plasma channel decreased as hTISIS temperatures went up. Nevertheless, even under these conditions, the sensitivity was at least around 2 times higher for this device than that achieved by using the Scott spray chamber.

In previous studies in which an organic sample has been continuously delivered to the nebulizer, the hTISIS has been operated at liquid flow rates on the order of $20\text{--}30\mu\text{L min}^{-1}$. Higher values of this variable would shorten the analysis time, although the plasma thermal state could degrade. In the present study, it was observed that the higher this variable, the higher the ion intensity (Figure 1), due to the increased amount of analyte reaching the plasma. Oxide ratios, in turn, did not vary significantly when increasing this variable, thus giving a proof that the plasma was not thermally degraded as increasing the liquid flow rate. Because deposits formation at the ICP-MS interface was favored at high Q_i values, $30\mu\text{L min}^{-1}$ was considered as a suitable value in terms of total evaporation of the sample in the chamber, analyte transport efficiency close to 100%, ICP-MS sensitivity and plasma thermal state.

Effect of hTISIS temperature and liquid flow rate on the matrix effects

ARTICLE

Journal Name

The influence of the hTISIS temperature and liquid flow rate on the matrix effects was also evaluated. For this purpose, the analysis of a wine sample was performed under various hTISIS temperatures and liquid flow rates. The undiluted sample was directly introduced into the ICP-MS and external calibration using aqueous standards containing 10% ethanol was applied. The concentrations found under each set of conditions were compared against those obtained using a reference analytical procedure, consisting in the microwave-assisted acid digestion, followed by ICP-MS analysis using a conventional sample introduction system (Scott spray chamber). The analytical results for three representative analytes (Mn, Mo and Pb) are reported in Table 2. At low hTISIS temperatures, quantitative data were statistically different to the expected ones according to the reference method. This was explained on the basis that the mass of analyte transported to the plasma depended on the matrix in the case of the hTISIS. However, both methods provided values not statistically different (highlighted in bold in Table 2, Student t-test at 95%-confidence level, Table S1) when working at 125°C and at 30 $\mu\text{L min}^{-1}$ liquid flow rate. In conclusion, under these conditions, matrix effects caused by wine were removed.

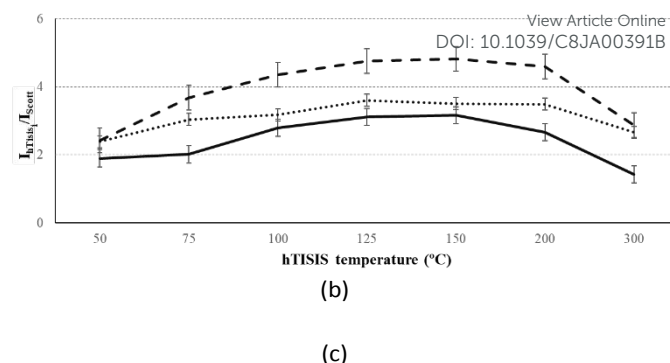
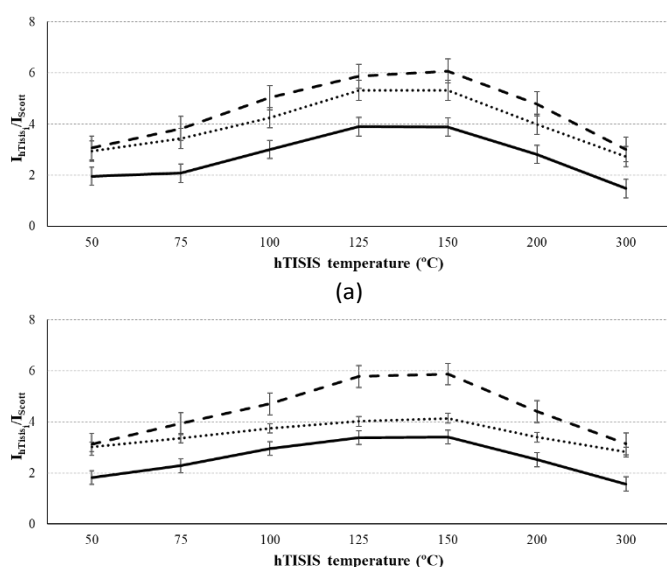


Figure 1. Ion intensity (normalized with respect to that obtained using the Scott spray chamber) as a function of the hTISIS temperature. Sample: Gutturnio wine spiked with the multielement standard solution at 50 $\mu\text{g kg}^{-1}$. Analytes: (a) ^{55}Mn ; (b) ^{111}Cd ; (c) ^{208}Pb . Liquid flow rate: 20 $\mu\text{L min}^{-1}$ (black line); 30 $\mu\text{L min}^{-1}$ (dotted line); 50 $\mu\text{L min}^{-1}$ (broken line).

An interesting trend highlighted in Table 2 was related with the fact that, globally speaking, at temperatures above 125°C, the accuracy of the determinations degraded. While the particular reasons for this phenomenon are not fully understood, it has been experimentally observed that the ions transversal diffusion in the plasma found at excessively high hTISIS temperatures may depend on the matrix composition.⁴⁸

Regarding the liquid flow rate, it was observed that, for most of the cases, the higher the value of this variable, the lower the obtained concentration (Table 2). This fact appeared to suggest a more intense ion transversal diffusion in the plasma at low rates (*i.e.*, 20 $\mu\text{L min}^{-1}$), whereas at high Q_i values, deposit formation at the interface in presence of wine samples, could decrease sensitivity, thus giving rise to lower analyte concentrations than the expected ones. Also in terms of matrix effects, 30 $\mu\text{L min}^{-1}$ appeared to be an optimal experimental condition.

Table 2. Mn, Mo and Pb concentrations obtained by hTISIS/ICP-MS analysis of a wine sample (Gutturnio) under different operating conditions (mean \pm 95%-confidence interval; values in $\mu\text{g kg}^{-1}$). Values not statistically different from those provided by the reference method* are highlighted in bold (Student t-test, 95%-confidence level).

hTISIS T(°C)	Mn			Mo			Pb		
	20 $\mu\text{L min}^{-1}$	30 $\mu\text{L min}^{-1}$	50 $\mu\text{L min}^{-1}$	20 $\mu\text{L min}^{-1}$	30 $\mu\text{L min}^{-1}$	50 $\mu\text{L min}^{-1}$	20 $\mu\text{L min}^{-1}$	30 $\mu\text{L min}^{-1}$	50 $\mu\text{L min}^{-1}$
50	815 \pm 53	733 \pm 37	937 \pm 60	10.8 \pm 1.4	3.94 \pm 0.17	3.71 \pm 0.22	10.20 \pm 0.35	5.53 \pm 0.11	4.01 \pm 0.51
75	1090 \pm 46	1069 \pm 23	875 \pm 31	6.51 \pm 0.94	5.94 \pm 0.31	4.33 \pm 0.22	9.22 \pm 0.64	4.78 \pm 0.36	3.09 \pm 0.13
100	1391 \pm 48	1315 \pm 39	1249 \pm 42	6.76 \pm 0.35	10.26 \pm 0.45	7.24 \pm 0.38	11.94 \pm 0.57	6.84 \pm 0.69	4.09 \pm 0.34
125	1420 \pm 170	1442 \pm 71	1585 \pm 98	11.42 \pm 0.56	13.71 \pm 0.48	12.41 \pm 0.57	8.34 \pm 0.35	5.87 \pm 0.32	4.24 \pm 0.36

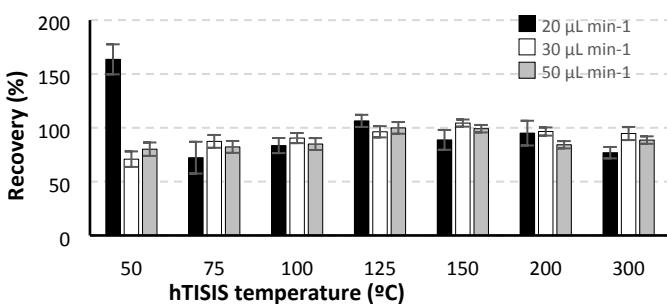
150	1556 ± 64	1539 ± 33	1394 ± 52	8.80 ± 0.71	14.00 ± 0.40	12.41 ± 0.30	12.57 ± 0.97	6.68 ± 0.13	4.06 ± 0.30
200	2290 ± 100	2160 ± 170	2000 ± 120	10.70 ± 0.81	13.45 ± 0.40	11.64 ± 0.37	14.6 ± 10	7.22 ± 0.74	5.53 ± 0.32
300	1050 ± 51	970 ± 32	947 ± 60	3.57 ± 0.28	10.74 ± 0.58	9.72 ± 0.32	4.00 ± 0.44	3.15 ± 0.29	2.67 ± 0.16
Reference method									
*		1521 ± 79			13.7 ± 1.1			4.83 ± 0.96	

* microwave-assisted acid digestion and ICP-MS analysis using a conventional sample introduction system at the liquid flow rate of 100 $\mu\text{L min}^{-1}$.

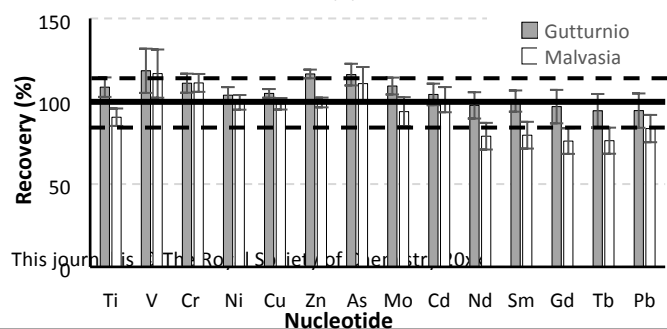
Method validation

The results obtained so far indicated that the hTISIS system operating at the temperature of 125°C and at a liquid flow rate of 30 $\mu\text{L min}^{-1}$ should provide optimal results in terms of sensitivity and mitigation of interferences. The first step for method validation was to perform recovery studies. In order to accomplish it, wine samples were spiked with a multielemental solution at a 50 $\mu\text{g kg}^{-1}$ level. External calibration was performed with a set of standards containing 10% in ethanol and the ICP-MS intensities for non-spiked samples were subtracted to those of the corresponding spiked ones. Data obtained for elements present at concentrations much higher than 50 parts per billion (e.g., Fe or Mn) were discarded because of the similarity of the signals found for spiked and non-spiked samples. Figure 2 summarizes the recoveries found under different operating conditions (Figure 2.a) and for two representative wine samples and several elements (Figure 2.b).

In concordance with the data shown in Table 2, an increase in the temperature led to an initial increase in the recovery that reached 100% at 125°C while at higher temperatures, recovery dropped. As regards the liquid flow rate, 30 $\mu\text{L min}^{-1}$ provided the most satisfactory results in terms of recovery. It may be observed that, for the selected operating conditions, 125°C and 30 $\mu\text{L min}^{-1}$, all the obtained data were included in between a 100 ± 10% range except for few elements such as Nd and Tb in Malvasia wine (Figure 2.b).



(a)



This journal is The Royal Society of Chemistry

Figure 2. (a) Recoveries as a function of the hTISIS operating conditions for Mo determination in the Gutturnio wine sample; (b) Recoveries with the hTISIS operated at 125°C and 30 $\mu\text{L min}^{-1}$ for two real wine samples. Solid line indicates values of 100% for the recovery, whereas the dotted lines indicated 90% and 110% values.

In order to further validate the method, the analysis of three wine samples was carried out using three different methods: undiluted wine analysis through the hTISIS, undiluted analysis using the Scott spray chamber, and analysis based on the microwave digestion and subsequent determination of the analyte concentration. Data were computed for all the considered analytes (Table 3). It can be seen that, with a few exceptions, the hTISIS provided concentrations that did not significantly differ from those reported by the digestion method (Table S2, Table S3 and Table S4), even for elements that were present at high levels such as Mn or Fe. Meanwhile, the conventional sample introduction system led to results poorly correlated with the data furnished by the reference method. This fact clearly suggested the appearance of matrix effects when the default sample introduction system was employed. For some elements (i.e., V, Cd, Nd, Sm, Gd and Tb), the content determined by the digestion method was lower than LOQ and, hence, the method validation was only based on the recovery results (see Figure 2). The accurate quantification of these elements was only possible with the hTISIS, because of the low LODs achieved (Table 4). Arsenic, in turn, provided unsatisfactory results that led to significantly different concentrations according to the methodology tested. However, as it has been pointed out recently, digestion (the reference method selected in the present work) is not a suitable method for the determination of this element in red wines.⁵³

The method detection limits (MDLs) were calculated according to the $3s_b$ criterion, where s_b was the standard deviation of ten consecutive blank measurements. Table 4 summarizes the MDLs values obtained for the hTISIS and the reference method (i.e., microwave-assisted acid digestion and ICP-MS analysis using a conventional sample introduction system) and compares them with values found by previously published studies. Dilution factors of these procedures are also reported. It can be seen that the MDLs achieved by the hTISIS method were significantly lower than those obtained by the reference method, with improvement factors ranging from 2 to 40. This result was a combination of the lower sample dilution

factor (direct injection against ~14-fold dilution) and the higher sensitivity previously highlighted (see Effect of hTISIS temperature and liquid flow rate on sensitivity section). However, these factors were partially balanced by the higher noise due to the high temperature of the hTISIS. Finally, the MDLs of the proposed method were close to or better than the values reported in the literature.^{36,37,39,40}

Table 3. Concentrations found for three wine samples using the reference microwave assisted digestion method, the conventional liquid sample introduction system and the hTISIS (mean \pm 95%-confidence interval; values in $\mu\text{g kg}^{-1}$).

	Tempranillo 2			Gutturnio			Rioja		
	MW Digestion	Conventional	hTISIS 125°C	MW Digestion	Conventional	hTISIS 125°C	MW Digestion	Conventional	hTISIS 125°C
Ti	29.7 \pm 8.5	30.3 \pm 2.9	44.2 \pm 2.3	39.07 \pm 0.13	43.7 \pm 1.8	37.4 \pm 1.8	52 \pm 47	84.3 \pm 9.1	46.4 \pm 2.8
V	< 1.5	0.305 \pm 0.024	1.467 \pm 0.090	< 1.5	ND	0.646 \pm 0.076	< 1.5	0.195 \pm 0.049	1.15 \pm 0.10
Cr	15.7 \pm 3.8	11.71 \pm 0.21	19.4 \pm 1.0	6 \pm 19	5.64 \pm 0.11	4.87 \pm 0.25	4 \pm 6	5.41 \pm 0.27	3.25 \pm 0.17
Mn	1704 \pm 42	1019 \pm 20	1723 \pm 100	1521 \pm 79	1328 \pm 32	1442 \pm 71	740.7 \pm 5.5	858 \pm 40	667 \pm 40
Fe	3320 \pm 230	2018 \pm 43	3460 \pm 190	1580 \pm 830	959.1 \pm 9.0	1229 \pm 48	1180 \pm 400	1421 \pm 64	1213 \pm 35
Ni	83 \pm 34	12.32 \pm 0.51	75.4 \pm 3.2	192.1 \pm 6.4	44.1 \pm 1.2	211.4 \pm 8.2	89 \pm 15	22.96 \pm 0.96	78.7 \pm 2.3
Cu	261 \pm 29	78.9 \pm 1.4	242 \pm 10	983 \pm 25	109.5 \pm 3.6	215.0 \pm 7.6	91 \pm 12	74.9 \pm 2.4	105.9 \pm 1.8
Zn	290 \pm 79	542 \pm 15	258 \pm 12	130 \pm 110	549 \pm 17	144.3 \pm 5.0	241 \pm 70	981 \pm 50	216.7 \pm 6.4
As	3.0 \pm 1.1	0.919 \pm 0.050	4.21 \pm 0.23	2.9 \pm 2.8	0.60 \pm 0.14	2.86 \pm 0.21	16.3 \pm 3.2	1.32 \pm 0.11	3.25 \pm 0.20
Mo	18.1 \pm 3.5	4.2 \pm 1.1	19.3 \pm 1.3	13.7 \pm 1.1	1.42 \pm 0.40	13.71 \pm 0.48	17.4 \pm 2.0	9.04 \pm 0.30	15.61 \pm 0.80
Cd	< 0.4	ND	0.390 \pm 0.043	< 0.4	ND	0.462 \pm 0.031	< 0.4	0.0261 \pm 0.0033	0.391 \pm 0.024
Nd	< 0.3	ND	< 0.02	< 0.3	0.043 \pm 0.015	0.0042	< 0.3	0.120 \pm 0.018	0.246 \pm 0.052
Sm	< 0.2	0.040 \pm 0.016	0.034 \pm 0.014	< 0.2	0.045 \pm 0.028	0.0055	< 0.2	0.057 \pm 0.014	0.0093
Gd	< 0.06	0.034 \pm 0.018	0.0018	< 0.06	0.0414 \pm 0.0091	0.0100 \pm 0.0018	< 0.06	0.0573 \pm 0.0068	0.0511 \pm 0.0034
Tb	< 0.03	0.031 \pm 0.033	0.0065	< 0.03	0.031 \pm 0.014	0.0113 \pm 0.0012	< 0.03	0.036 \pm 0.013	0.0946 \pm 0.0054
Pb	13.50 \pm 0.49	6.12 \pm 0.11	12.20 \pm 0.60	4.83 \pm 0.96	3.08 \pm 0.65	5.87 \pm 0.32	23.2 \pm 6.9	11.87 \pm 0.35	18.21 \pm 0.48

ND: Not detected

Table 4. Detection limits of the developed method, the reference method based on microwave-assisted acid digestion and other ICP-based published methods (values in $\mu\text{g kg}^{-1}$).

Dilution factor	hTISIS method	Reference method *	Ref. 39	Ref. 40	Ref. 36	Ref. 37
	Undiluted	14	3	3	10	10
⁴⁷ Ti	0.4	1.4	1.6	0.7	0.16	5
⁵¹ V	0.015	0.5	0.07	0.03	0.12	0.7
⁵² Cr	0.14	0.5	0.2	0.7	15	
⁵⁵ Mn	0.17	0.5	0.07	0.2	0.7	
⁵⁶ Fe	4	25				
⁶⁰ Ni	0.16	0.6	1.0	0.3	3	1.0
⁶³ Cu	0.18	1.0	0.07	0.15	0.8	10
⁶⁶ Zn	3	0.5	0.05	0.8	2	
⁷⁵ As	0.05	0.6	0.02	0.04		3
⁹⁵ Mo	0.13	1.3	0.09	0.2		
¹¹¹ Cd	0.03	0.13	0.03	0.02		
¹⁴⁶ Nd	0.007	0.1		0.006		1.2
¹⁴⁷ Sm	0.002	0.08	0.006	0.006		

¹⁵⁷ Gd	0.002	0.02	0.003	0.003	0.9
¹⁵⁹ Tb	0.002	0.017			
²⁰⁸ Pb	0.02	0.15	0.015	0.02	0.12

* microwave-assisted acid digestion and ICP-MS analysis using a conventional sample introduction system.

Method applicability to routine analysis

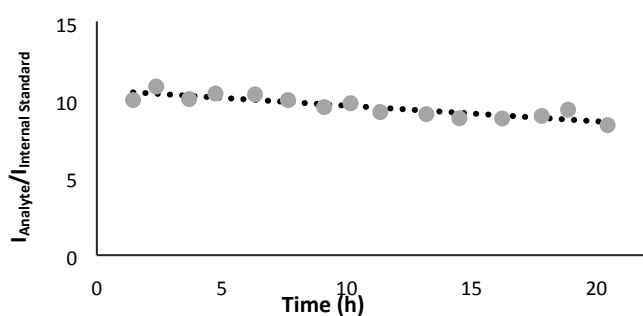
The hTISIS was applied for the first time to perform analysis of wine samples on a routine basis under a continuous sample aspiration regime. This sample introduction system involves several advantages: First, the use of hTISIS allows the minimization of sample consumption, since it works at a liquid flow rate of a few microliters per minute. More importantly, no residues are generated once the analysis is completed. Note that the hTISIS did not contain any drain exit. Moreover, the method does not require any sample preparation (except filtering), thereby reducing contamination problems, potential loss of analytes and the overall analysis time. In fact, the whole analytical procedure can be accomplished in 7 minutes per sample, whereas the microwave-assisted acid digestion, cooling, and analysis require about 40 minutes.

The method applicability to routine analyses was tested by processing about 70 samples (including the wine samples, standards and QC) consecutively, throughout an automatized 20-hours analytical run. A QC standard at the concentration of $100 \mu\text{g kg}^{-1}$ ($10 \mu\text{g kg}^{-1}$ for rare earth elements) was analyzed every hour to assess a possible drift in the analytical signals. Representative trends are shown in Figure 3. Regression analysis⁵⁴ of QC data pointed out significant linear trends for V, Cr, Ni, Cu, Cd and Pb (95%-confidence level, Table S5); however, their overall variation was within 20%, that was acceptable for routine analysis purposes. Moreover, the regression parameters obtained from QC data can be used for correcting the analytical results, according to the following equation:

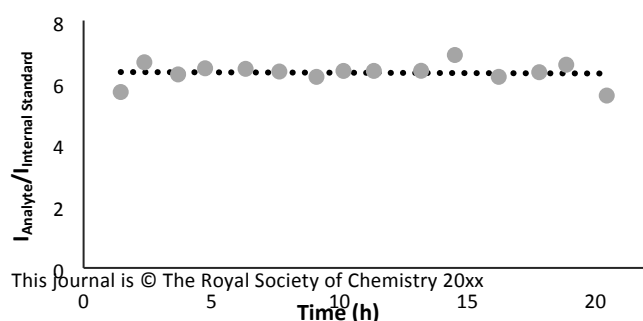
$$x_c(i) = x(i) - b \cdot i \quad \text{Equation 1}$$

where i is the position of the result in the analytical run; b is the slope of the linear regression; $x(i)$ is the analytical result at the position i and, $x_c(i)$ is the corresponding corrected result. After data processing, the variation of the concentration for the QC samples throughout the analytical run was better than 10%.

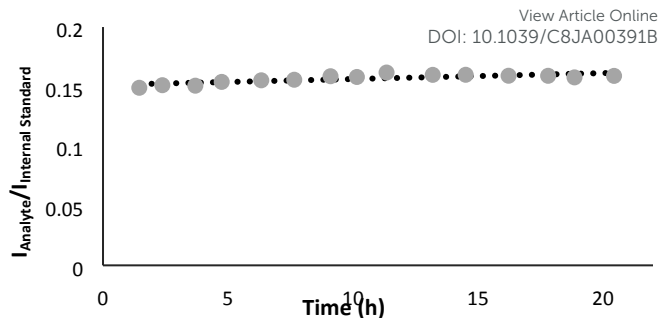
Finally, it is important to note that, despite the organic matrix of the processed samples, carbon deposits were not observed in the spectrometer components at the end of the analytical sequence, likely due to the low liquid flow rate applied.



(a)



(b)



(b)

(c)

Figure 3. Temporal variation of the analytical signal for the QC standard. (a) Cr; (b) Mn; (c) Cd.

Analytical results

The concentrations of trace elements in ten representative wine samples are reported in Table 5, in order to show the suitability of the proposed method for the analysis of real samples. According to the found concentrations, the elements can be divided into three groups. Elements such as Fe, Mn and Zn were present at relatively high concentration, ranging from 0.1 to 3.5 mg kg^{-1} . As these elements are directly related to external practices, no differences have been found between Italian and Spanish wines. Other trace elements (e.g. Cr, Pb and V) occurred at the 1 – $100 \mu\text{g kg}^{-1}$ concentration, showing a great variation among samples with the same geographical origin and no significant difference between the cultivation regions. This behavior has been previously discussed by Pohl.³ Finally, Cd and rare earth elements were found at the sub- $\mu\text{g kg}^{-1}$ concentration level, without marked differences among the regions.

Conclusions

The application of hTISIS working at $30 \mu\text{L min}^{-1}$ and 125°C in combination with ICP-MS allows the direct determination of trace elements in wine samples, with minimum sample manipulation and reduced analysis time. Under the optimal conditions, matrix effects are efficiently mitigated, and the limits of detection improved in comparison with conventional systems. The analysis time is about 6-times lower than that required by the procedures based on microwave-assisted acid digestion. In addition, due to the low amount of sample required and its total introduction into the ICP source, the waste generation is minimized, bringing the laboratory closer to the concept of green chemistry.

The new procedure is hence proposed as a suitable alternative for the routine analysis of wine samples, as demonstrated by the continuous automatic analysis of a series of real samples in a 20-hours long analytical session.

The list of analytes for which satisfactory results have been achieved so far comprises many trace elements of interest, including heavy metals of toxicological concerns and proxies of provenience such as the rare earth elements. Future work will

be aimed at enlarging the number of analytes, in order to provide a more complete elemental fingerprint of wine samples.

Table 5. Trace element concentrations in wine samples (mean \pm 95%-confidence interval).

Analyte	Gutturnio (Italy)	Malvasia (Italy)	Ortrugo (Italy)	Cabernet S. (Italy)	Cortese (Italy)	Monastrell (Spain)	Tempranillo 1 (Spain)	Tempranillo 2 (Spain)	Rioja (Spain)	Alicante (Spain)
Ti	37 \pm 2	73 \pm 4	125 \pm 2	138 \pm 12	93 \pm 4	88 \pm 5	88 \pm 8	44 \pm 2	46 \pm 3	80 \pm 2
V	0.65 \pm 0.08	12.1 \pm 0.8	12.0 \pm 0.7	18 \pm 3	45.2 \pm 0.6	12.9 \pm 0.7	12 \pm 1	1.47 \pm 0.09	1.2 \pm 0.1	20.7 \pm 0.5
Cr	4.9 \pm 0.2	36 \pm 1	80 \pm 1	32 \pm 1	26.7 \pm 0.8	28 \pm 2	27 \pm 2	19 \pm 1	3.3 \pm 0.2	25.7 \pm 0.8
Mn	1442 \pm 71	1182 \pm 40	1496 \pm 16	1102 \pm 173	412 \pm 10	933 \pm 54	988 \pm 63	1723 \pm 100	667 \pm 40	779 \pm 20
Fe	1229 \pm 48	714 \pm 42	701 \pm 12	2421 \pm 384	440 \pm 9	1423 \pm 99	1280 \pm 96	3457 \pm 186	1213 \pm 35	1158 \pm 26
Ni	211 \pm 8	44 \pm 1	61.4 \pm 0.8	42 \pm 1	29.6 \pm 0.6	28 \pm 2	30.2 \pm 0.9	75 \pm 3	79 \pm 2	25.7 \pm 0.7
Cu	215 \pm 8	182 \pm 7	1954 \pm 68	268 \pm 28	214 \pm 10	102 \pm 6	89 \pm 14	242 \pm 10	106 \pm 2	29 \pm 2
Zn	144 \pm 5	685 \pm 32	2505 \pm 77	158 \pm 9	266 \pm 9	585 \pm 35	523 \pm 84	258 \pm 12	216 \pm 6	601 \pm 17
As	2.9 \pm 0.2	3.8 \pm 0.2	4.0 \pm 0.2	3.5 \pm 0.6	3.3 \pm 0.1	2.9 \pm 0.2	2.5 \pm 0.4	4.2 \pm 0.2	3.3 \pm 0.2	2.4 \pm 0.1
Mo	13.7 \pm 0.5	17 \pm 3	25 \pm 2	25 \pm 3	42 \pm 1	60 \pm 6	32 \pm 2	19.3 \pm 1.3	15.6 \pm 0.8	24.4 \pm 0.5
Cd	0.46 \pm 0.03	0.32 \pm 0.02	< 0.03	< 0.03	0.14 \pm 0.02	< 0.03	< 0.03	0.39 \pm 0.04	0.39 \pm 0.02	< 0.03
Nd	0.026 \pm 0.004	0.13 \pm 0.02	0.09 \pm 0.01	1.6 \pm 0.2	2.8 \pm 0.8	0.09 \pm 0.02	0.057 \pm 0.009	< 0.02	0.25 \pm 0.05	0.16 \pm 0.03
Sm	0.072 \pm 0.006	0.11 \pm 0.02	0.059 \pm 0.007	0.39 \pm 0.06	0.64 \pm 0.04	0.09 \pm 0.02	0.050 \pm 0.009	0.03 \pm 0.01	0.263 \pm 0.009	0.062 \pm 0.009
Gd	0.010 \pm 0.002	0.36 \pm 0.05	0.08 \pm 0.01	0.37 \pm 0.06	0.59 \pm 0.3	0.10 \pm 0.01	0.05 \pm 0.01	0.007 \pm 0.002	0.051 \pm 0.003	0.11 \pm 0.01
Tb	0.011 \pm 0.001	0.10 \pm 0.01	0.042 \pm 0.005	0.09 \pm 0.01	0.15 \pm 0.02	0.07 \pm 0.01	0.038 \pm 0.008	0.044 \pm 0.007	0.095 \pm 0.005	0.038 \pm 0.004
Pb	5.8 \pm 0.3	19 \pm 2	13.9 \pm 0.9	35 \pm 3	9.4 \pm 0.4	37 \pm 2	10.9 \pm 0.2	12.2 \pm 0.6	18.2 \pm 0.5	17 \pm 1

Conflicts of interest

There are no conflicts to declare.

References

- J. Šperková and M. Suchánek, *Food Chem.*, 2005, **93**, 659-663.
- J.G. Ibáñez, A. Carreón-Álvarez, M. Barcena-Soto and N. Casillas, *J. Food Comp. Anal.*, 2008, **21**, 672-683.
- P. Pohl, *Trends Anal. Chem.*, 2007, **26**, 941-949.
- S.M. Rodrigues, M. Otero, A.A. Alves, J. Coimbra, M.A. Coimbra, E. Pereira and A.C. Duarte, *J. Food Comp. Anal.*, 2011, **24**, 548-562.
- J. Karasinski, J.C.T. Elguera, A.A.G. Ibarra, K. Wrobel, E. Bulska and K. Wrobel, *Anal. Lett.*, 2018, **51**, 2643-2657.
- B. Tariba, *Biol. Trace Elem. Res.*, 2011, **144**, 143-156.
- G. Grindlay, J. Mora, L. Gras and M.T.C. de Loos-Vollebregt, *Anal. Chim. Acta*, 2011, **691**, 18-32.
- Compendium of international methods of wine and must analysis*, International Organisation of Vine and Wine, 2012.
- L. Fernández-López, B. Gómez-Nieto, M.J. Gismera, M.T. Sevilla and J.R. Procopio, *Spectrochim. Acta B*, 2018, **147**, 21-27.
- F.D. Bora, C.L. Bunea, T. Rusu and N. Pop, *Chem. Cent. J.*, 2015, **9**, 19-31.
- S. Kinaree and S. Chanthai, *Chem. Pap.*, 2014, **68**, 342-351.
- S. Santos, N. Lapa, A. Alves, J. Morais and B. Mendes, *J. Environ. Sci. Health. Part B*, 2013, **48**, 364-375.
- C. Calin, G. Scaeteanu, M. Pele, L. Ilie, O. Pantea and D. Bombos, *Rev. Chim-Bucharest*, 2012, **63**, 1062-1064.
- F. Papageorgiou, K. Karampatea, A.C. Mitropoulos and G.Z. Kyzas, *Int. J. Environ. Sci. Technol.*, 2018, 1-10.
- V. Ivanova-Petropulos, B. Balabanova, E. Bogeva, T. Frentiu, M. Ponta, M. Senila, R. Gulaboski and F.D. Irimie, *Food Anal. Methods*, 2017, **10**, 459-468.
- A. Chen, S.L. Chen, Y.H. Wu, Y. Shao and C.L. Zhang, *Adv. Mat. Res.*, 2014, **1033-1024**, 658-662.
- N.O. Đorđević, B. Pejcin, M.M. Novaković, D.M.d. Stanković, J.J. Mutić, S.B. Pajović and V.V. Tešević, *Nat. Prod. Res.*, 2018, **32**, 247-251.
- A.J. Gutiérrez, C. Rubio, I.M. Moreno, A.G. González, D. González-Weller, N. Bencharik, A. Hardisson and C. Revert, *Food Chem. Toxicol.*, 2017, **108**, 10-18.
- D.D. Karatas, F. Aydin, I. Aydin and H. Karatas, *Czech Journal of Food Sciences*, 2015, **33**, 228-236.
- X.D. Pan, J. Tang, Q. Chen, P.G. Wu and J.L. Han, *Eur. Food Res. Technol.*, 2013, **236**, 531-535.
- M. Álvarez, I.M. Moreno, S. Pichardo, A.M. Cameán and A. Gustavo-González, *Food Chem.*, 2012, **1**, 309-313.
- A. Ziola- Frankowska and M. Frankowski, *Food Anal. Methods*, 2017, **10**, 180-190.
- S. Pepi and C. Vaccaro, *Environ. Geochem. Hlth*, 2018, **40**, 833-847.
- K. Guo, S. Wells, F.X. Han, Z. Arslan, H. Sun and J. Zhang, *Water Air Soil Poll.*, 2017, **228**, 76-82.

- 25 S. Pepi, L. Sansone, M. Chicca, E. Morrocchino and C. Vaccaro, *Environ. Monit. Assess.*, 2016, **188**, 477-482.
- 26 C. Avram, C. Voica, A. Hosu, C. Cimpoiu and C. Măruțoiu, *Revue Roumanie de Chimie*, 2014, **59**, 1009-1019.
- 27 C. Avram, D.A. Magdas, C. Voica, G. Cristea, C. Cimpoiu, A. Hosu and C. Marutoiu, *Anal. Lett.*, 2014, **47**, 641-653.
- 28 M. Di Martino, D. Ciavardelli, F. Di Giacomo, C. Civitarese and A. Cichelli, *Agro Food Ind. HiTech*, 2013, **24**, 30-34.
- 29 H. Hopfer, J. Nelson, A.E. Mitchell, H. Heymann and S.E. Ebeler, *J. Anal. At. Spectrom.*, 2013, **28**, 1288-1291.
- 30 V.L. Dressler, C.M.M. Santos, F.G. Antes, F.R.S. Bentlin, D. Pozebon, and E.M.M. Flores, *Food Anal. Methods*, 2012, **5**, 505-511.
- 31 S.M. Rodrigues, M. Otero, A.A. Alves, J. Coimbra, M.A. Coimbra, E. Pereira and A.C. Duarte, *J. Food Comp. Anal.*, 2011, **24**, 548-562.
- 32 A.W. Boorn and R.F. Browner, *Inductively Coupled Plasma Emission Spectroscopy*; NewYork, 1987.
- 33 A.W. Boorn and R.F. Browner, *Anal. Chem.*, 1982, **54**, 1402-1410.
- 34 C.K. Pan, G.X. Zhu and R.F. Browner, *J. Anal. At. Spectrom.*, 1990, **5**, 537-542.
- 35 C. Voica, A. Dehelean and A. Pamula, *J. Phys. Conf. Ser.*, 2009, **182**, 1-5.
- 36 A. González. S. Armenta, A. Pastor and M. de la Guardia, *J. Agric. Food Chem.*, 2008, **56**, 4943-4954.
- 37 V.S. Selih, M. Sala and V. Drgan, *Food Chem.*, 2014, **153**, 414-423.
- 38 I. Rodushkin, F. Ödman and P.K. Appelblad, *J. Food Comp. Anal.*, 1999, **12**, 243-257.
- 39 H. Hopfer, J. Nelson, T.S. Collins, H. Heymann and S.E. Ebeler, *Food Chem.*, 2015, **172**, 486-496.
- 40 J. Godshaw, H. Hopfer, J. Nelson and S.E. Ebeler, *Molecules*, 2017, **22**, 1609-1623. VIEW ARTICLE ONLINE
DOI: 10.1039/C8JA00391B
- 41 A.E. Martin, R.J. Watling and G.S. Lee, *Food Chem.*, 2012, **133**, 1081-1089.
- 42 I.M. Moreno, D. González-Weller, V. Gutierrez, M. Marino, A.M. Cameán, A.G. González and A. Hardisson, *Microchem. J.*, 2008, **88**, 56-61.
- 43 G. Grindlay, J. Mora, L. Gras and M.T.C. de Loos-Vollebregt, *Anal. Chim. Acta*, 2009, **652**, 154-160.
- 44 G. Grindlay, J. Mora, S. Maestre and L. Gras, *Anal. Chim. Acta*, 2008, **629**, 24-37.
- 45 G. Grindlay, J. Mora, M.T.C. de Loos-Vollebregt and F. Vanhaecke, *Talanta*, 2014, **128**, 379-385.
- 46 R. Sánchez, J. L. Todolí, C.P. Lienemann and J. M. Mermet, *J. Anal. At. Spectrom.*, 2012, **27**, 937-945.
- 47 F. Ardini, M. Grotti, R. Sánchez and J.L. Todolí, *J. Anal. At. Spectrom.*, 2012, **27**, 1400-1404.
- 48 C. Sánchez, C.P. Lienemann and J. L. Todolí, *Spectrochim. Acta B*, 2016, **124**, 99-108.
- 49 C. Sánchez, E. Bolea-Fernández, M. Costas-Rodríguez, C.P. Lienemann, J.L. Todolí and F. Vanhaecke, *J. Anal. At. Spectrom.*, 2018, **33**, 481-490.
- 50 R.I. Botto and J.J. Zhu, *J. Anal. At. Spectrom.*, 1994, **9**, 905-912.
- 51 R.I. Botto and J.J. Zhu, *J. Anal. At. Spectrom.*, 1996, **11**, 675-681.
- 52 C. Sánchez, C.P. Lienemann and J. L. Todolí, *Spectrochim. Acta B*, 2016, **115**, 16-24.
- 53 E.P. Pérez-Álvarez, R. García, P. Barrulas, C. Dias, M.J. Cabrita, T. Garde-Cerdán, *Food Chem.*, 2019, **270**, 273-280.
- 54 *EURACHEM Guide: The fitness for purpose of analytical methods: A laboratory guide to method validation and related topics*; LGC Teddington, 1998.

Table S1. Calculated t-values and s-values for the comparison between the analytical results obtained by hTISIS/ICP-MS analysis under different operating conditions and by a reference method (microwave-assisted acid digestion and ICP-MS analysis using a conventional sample introduction system). Values of t lower than the critical t-value for 9 degrees of freedom and 95%-confidence level are highlighted in bold.

hTISIS T(°C)	Mn						Mo						Pb					
	20 $\mu\text{L min}^{-1}$		30 $\mu\text{L min}^{-1}$		50 $\mu\text{L min}^{-1}$		20 $\mu\text{L min}^{-1}$		30 $\mu\text{L min}^{-1}$		50 $\mu\text{L min}^{-1}$		20 $\mu\text{L min}^{-1}$		30 $\mu\text{L min}^{-1}$		50 $\mu\text{L min}^{-1}$	
	t	s	t	s	t	s	t	s	t	s	t	s	t	s	t	s	t	s
50	16	62	22	52	13	66	3.0	1.3	21.8	0.6	22.0	0.6	12.4	0.6	1.8	0.5	1.8	0.7
75	10	57	14	46	18	50	10.0	1.0	16.4	0.7	20.6	0.6	8.2	0.8	0.2	0.6	4.6	0.5
100	3	59	5	53	7	55	14.3	0.7	6.6	0.7	13.1	0.7	13.9	0.7	3.5	0.8	1.8	0.6
125	1.0	151	1.5	73	1.0	93	4.1	0.8	0.1	1.1	2.3	0.8	8.1	0.6	2.3	0.6	1.4	0.6
150	0.7	69	0.5	51	3	61	8.1	0.9	0.7	0.7	2.7	0.7	11.1	1.0	4.7	0.5	1.9	0.6
200	11	95	6	148	6	109	4.5	0.9	0.4	0.7	4.1	0.7	13.4	1.0	4.1	0.8	1.6	0.6
300	10	60	16	50	12	66	21.7	0.7	5.2	0.8	8.3	0.7	1.9	0.6	4.1	0.6	5.7	0.5

Table S2. Calculated t values, degree of freedom (D.F.), the critical t value (95%-confidence level) and equations employed to calculate t and s. Values of t lower than the critical t-value level are highlighted in bold. Sample: Tempranillo 2.

		⁴⁷ Ti	⁵¹ V	⁵² Cr	⁵⁵ Mn	⁵⁶ Fe	⁶⁰ Ni	⁶³ Cu	⁶⁶ Zn	⁷⁵ As	⁹⁵ Mo	¹¹¹ Cd	¹⁴⁶ Nd	¹⁴⁷ Sm	¹⁵⁷ Gd	¹⁵⁹ Tb	²⁰⁸ Pb
Conventional system	t [#]	0.14	NC	4.5	66	23.7	9.1	28	13	8.9	17	NC	NC	NC	NC	NC	64
	D.F. [§]	2	NC	2	3	2	2	2	2	2	2	NC	NC	NC	NC	NC	2
hTISIS	t [#]	7.2	NC	4.1	0.94	2.2	1.0	3.7	1.8	4.3	1.4	NC	NC	NC	NC	NC	8.3

D.F.^s 2 NC 2 6 4 2 2 2 2 2 2 NC NC NC NC NC NC

View Article Online
DOI: 10.1039/C8JA00391B

$$t = \frac{(\bar{x}_1 - \bar{x}_2)}{\sqrt{\frac{s_1^2}{n_1} + \frac{s_2^2}{n_2}}}, DF = \frac{\left(\frac{s_1^2}{n_1} + \frac{s_2^2}{n_2}\right)}{\left(\frac{s_1^2}{n_1^2(n_1-1)} + \frac{s_2^2}{n_2^2(n_2-1)}\right)}$$

The F-test demonstrated that the variances of the procedures were not statistically comparable; NC: Not Calculated.

Table S3. Calculated t values, degree of freedom (D.F.), the critical t value (95%-confidence level) and equations employed to calculate t and s. Values of t lower than the critical t-value level are highlighted in bold. Sample: Gutturño.

		⁴⁷ Ti	⁵¹ V	⁵² Cr	⁵⁵ Mn	⁵⁶ Fe	⁶⁰ Ni	⁶³ Cu	⁶⁶ Zn	⁷⁵ As	⁹⁵ Mo	¹¹¹ Cd	¹⁴⁶ Nd	¹⁴⁷ Sm	¹⁵⁷ Gd	¹⁵⁹ Tb	²⁰⁸ Pb
Conventional system	t [#]	14	NC	0.17	10	3.2	98	150	17	3.6	44	NC	NC	NC	NC	NC	6.8
	D.F. ^s	5	NC	2	2	2	2	2	2	2	2	NC	NC	NC	NC	NC	3
hTISIS	t [#]	2.5	NC	0.35	2.7	1.8	9.2	130	0.78	0.16	0.21	NC	NC	NC	NC	NC	4.2
	D.F. ^s	5	NC	2	4	2	5	2	2	2	2	NC	NC	NC	NC	NC	2

$$t = \frac{(\bar{x}_1 - \bar{x}_2)}{\sqrt{\frac{s_1^2}{n_1} + \frac{s_2^2}{n_2}}}, DF = \frac{\left(\frac{s_1^2}{n_1} + \frac{s_2^2}{n_2}\right)}{\left(\frac{s_1^2}{n_1^2(n_1-1)} + \frac{s_2^2}{n_2^2(n_2-1)}\right)}$$

The F-test demonstrated that the variances of the procedures were not statistically comparable; NC: Not Calculated.

Table S4. Calculated t values, degree of freedom (D.F.), the critical t value (95%-confidence level) and equations employed to calculate t and s. Values of t higher than the critical t-value level are highlighted in bold. Sample: Rioja.

		⁴⁷ Ti	⁵¹ V	⁵² Cr	⁵⁵ Mn	⁵⁶ Fe	⁶⁰ Ni	⁶³ Cu	⁶⁶ Zn	⁷⁵ As	⁹⁵ Mo	¹¹¹ Cd	¹⁴⁶ Nd	¹⁴⁷ Sm	¹⁵⁷ Gd	¹⁵⁹ Tb	²⁰⁸ Pb
Conventional system	t [#]	2.9	NC	1.1	16	2.5	19	6.0	39	20	18	NC	NC	NC	NC	NC	6.6
	D.F. ^s	2	NC	2	4	2	2	2	3	2	2	NC	NC	NC	NC	NC	2
hTISIS	t [#]	0.53	NC	0.40	10	0.41	3.2	5.5	1.5	18	3.7	NC	NC	NC	NC	NC	2.7
	D.F. ^s	2	NC	2	4	2	2	2	2	2	2	NC	NC	NC	NC	NC	2

$$t = \frac{(\bar{x}_1 - \bar{x}_2)}{\sqrt{\frac{s_1^2}{n_1} + \frac{s_2^2}{n_2}}}, DF = \frac{\left(\frac{s_1^2}{n_1} + \frac{s_2^2}{n_2}\right)}{\left(\frac{s_1^2}{n_1^2(n_1-1)} + \frac{s_2^2}{n_2^2(n_2-1)}\right)}$$

The F-test demonstrated that the variances of the procedures were not statistically comparable; NC: Not Calculated.

Table S5. Calculated slope, s_{Slope} and t-values for the temporal trends of QC data. Values of t higher than the critical t-value for 13 degrees of freedom and 95%-confidence level are highlighted in bold.

	⁴⁷ Ti	⁵¹ V	⁵² Cr	⁵⁵ Mn	⁵⁶ Fe	⁶⁰ Ni	⁶³ Cu	⁶⁶ Zn	⁷⁵ As	⁹⁵ Mo	¹¹¹ Cd	¹⁴⁶ Nd	¹⁴⁷ Sm	¹⁵⁷ Gd	¹⁵⁹ Tb	²⁰⁸ Pb
slope	-	-	-	-	-	-	-	-	-	-	0.0005	0.00008	0.00010	0.0000	-	-
s _{Slope}	0.0007	0.008	0.015	0.015	0.09	0.006	0.03	0.005	0.008	0.00003	0.0001	0.00009	0.00008	0.0002	0.0006	0.016
t	1.346	4.749	6.783	0.166	0.54	6.754	3.99	2.073	0.996	0.182	4.780	0.884	1.274	0.212	1.390	2.460